Improving Arrays for Multi-Angle Swath Bathymetry

John S. Bird
Sabir Asadov
Paul Kraeutner
School of Engineering Science
Simon Fraser University
8888 University Drive
Burnaby, B.C. Canada
V5A 1S6
jbird@sfu.ca

***Abstract*-Multi-angle swath bathymetry sonar systems use the range and estimates of the angle of signal arrival to determine bottom depth. The accuracy of angle of arrival estimates is influenced by a number of factors including noise levels, the presence of mulitpath arrivals, signal bandwidth, pulse length etc. Angle estimation accuracy is also affected by the integrity of the transducer array employed to receive the returning signals. This paper addresses some of the issues associated with transducer design for multi-angle swath bathymetry systems including inter-element crosstalk and housing interactions. Beampatterns and relative angle responses are presented for transducer arrays that show evidence of crosstalk and housing interactions. It is shown that the crosstalk and housing interactions can be reduced through the use of different inter-element materials and housing configurations. Beampatterns and relative angle responses are presented for an improved array and compared to the previous patterns and phase responses. The discussion and experimental results are limited to arrays constructed with piezo-ceramic bars resonant at 300 kHz, and intended for shallow water use.**

I. INTRODUCTION

Multi-angle Swath Bathymetry (MASB) employs a multi-element array to estimate the directions of arrival (DOA) of multiple signals. Specifically, an MASB system can estimate as many as N-1 signal directions with an N element array. Because MASB systems estimate multiple angles of arrival they can operate in more complex situations than interferometric systems that estimate only one angle of arrival. For example, in shallow water applications where a surface bounce mulitpath is present the MASB system will estimate the angle of arrival of both the bottom return and the multipath return. Whereas the interferometric system's estimate of the angle of arrival of the bottom return will be hampered by the presence of the multipath return. In addition, MASB systems have certain advantages and disadvantages compared with mulitbeam systems and these are outlined in [1]. The advantages include; higher achievable crosstrack resolution, wider useable swath coverage, inherent co-location of both imagery and bathymetry data, smaller size, and lower complexity. The disadvantages are; lower resolution near nadir, and less ability to resolve complex target geometries.

In applications suited to the MASB configuration, the issue of angle estimation accuracy arises. There are a number of factors that influence angle estimation accuracy including, system noise, angular spread of target, and bandwidth of signal. A fourth issue that influences estimation accuracy is the integrity of the transducer array and it is this issue that is the focus of this paper.

In the process of estimating angles of arrival it is necessary to assume some signal model for the acoustic transducer array. Typically it is assumed the array consists of N acoustic elements mounted vertically with respect to one another as shown in Fig. 1. It is assumed in the processing that each element's beampattern is identical to any other element's beampattern. In other words, there is no crosstalk between elements or structures within the array or outside the array that would tend to make the beampatterns different from one another. The condition of similar beampatterns does not necessarily mean there is no crosstalk, but that the crosstalk, if present, is such that the element beampatterns are identical. If there is no crosstalk the similarity condition is assured. The beampattern similarity condition is difficult to achieve in practice and therefore angle estimates are usually corrupted to the extent the assumption is violated.

In this paper the issue of array integrity is addressed within the context of MASB applications. First the influence of element crosstalk and structure interaction on angle estimates is discussed. It is shown how crosstalk and structure interactions affect the beampatterns, relative phase, and ultimately the estimate of the arrival angle. To illustrate the array's performance a coherent beampattern for each element is constructed and the resulting relative angle shown for a specific level of crosstalk. Next, the physical construction of three arrays is described with a focus on crosstalk mitigation. The coherent beampatterns and relative phases are presented for each array. Crosstalk and structure

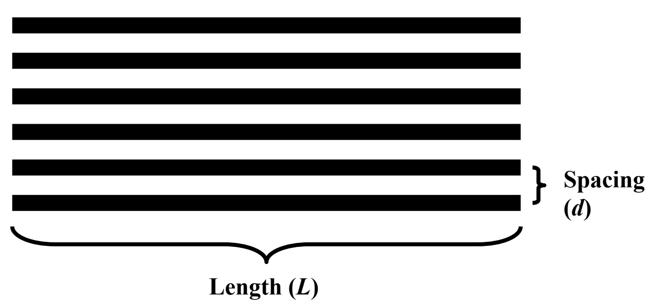

Fig. 1. Typical configuration for an array used for multi-angle swath bathymetry.

0-933957-31-9

interactions are discussed. The inverse Fourier transform of the coherent beampattern is shown to provide information about the aperture function across the array that produces the far field beampatterns. These aperture functions indicate that the housing structure of the array can play an important role in determining the integrity of the array. Finally, the angle estimation performance of the three arrays is compared and conclusions drawn about the effect of crosstalk on bottom estimation accuracy.

II. CROSSTALK AND STRUCTURE INFLUENCES

In this section a simple model for crosstalk and structural influences on the output signals of an array is presented. The array is assumed to be a linear array of three elements for illustration, but the formulation is easily extended to an arbitrary number of elements. It is assumed that each array element interacts directly with its neighbour and indirectly with the other elements. Therefore, the output signals may be written

$$\begin{aligned} x_1 &= s_1 + bx_2 + 0 \\ x_2 &= bx_1 + s_2 + bx_3 \\ x_3 &= 0 + bx_2 + s_3 \end{aligned} \quad (1)$$

where x_i is the output signal of the i^{th} element, s_i is the incident signal on the i^{th} element, and b is the coupling factor. Therefore,

$$\begin{bmatrix} 1 & -b & 0 \\ -b & 1 & -b \\ 0 & -b & 1 \end{bmatrix} \begin{bmatrix} x_1 \\ x_2 \\ x_3 \end{bmatrix} = \begin{bmatrix} s_1 \\ s_2 \\ s_3 \end{bmatrix} \quad (2)$$

or

$$Ax = s \quad (3)$$

where A is the interaction matrix, x is the vector of output signals, and s is the signal vector across the array, namely

$$s = \begin{bmatrix} 1 \\ \exp(j\theta) \\ \exp(j2\theta) \end{bmatrix} \quad (4)$$

where θ is the relative electrical angle.

The array outputs from the signal vector are determined from (3) as

$$x = A^{-1}s \quad (5)$$

where A^{-1} is defined as the crosstalk matrix. More generally, for N elements A is a band matrix with diagonal elements equal to one and upper and lower diagonal elements equal to $-b$. The crosstalk matrix is the inverse of this band matrix.

It is evident from (3) and the form of A that crosstalk can be undone mathematically if A is known. Therefore crosstalk of this kind is potentially not very serious. In practice, however, the situation is rarely so simple. And even if it were, the matrix operation in (3) would introduce element-to-element correlation in the independent front-end noise on each element, and thereby influence the angle estimates.

A more serious problem, however, is that the signals on all the elements or structures producing crosstalk are not usually observable. For example, if the array is composed of four elements but the outer two are not observed we only have x_2 and x_3 and from these alone we cannot reconstruct s_2 and s_3. We need x_1 and x_4 as well as the full matrix A. Unobserved elements might be dummy elements used to reduce edge effects or indeed any other structures such as the edge of the housing.

The purpose, therefore, for introducing the crosstalk model above is not to describe in detail the effect of crosstalk in real situations, but instead to provide a bases from which to start the discussion on crosstalk. Figure 2 presents the beampatterns for a six element array (spacing λ/2, were λ is the wavelength) with an element coupling factor of $0.4\angle 120^{o}$ (i.e. $0.4\exp(j2\pi/3)$). Also shown is the expected pattern for no crosstalk (dashed line). Note that the pattern shaping function of cos(ϕ) (where ϕ is the physical angle of arrival) associated with a soft baffle has been applied to the patterns [2].

The patterns for the corresponding elements on each side of the array are mirror images of each other because of the symmetry of the array. The ripples in the patterns are due to the crosstalk as it combines constructively or destructively depending on signal incident angle. Similar ripples are evident in the relative angle plots shown in Fig. 3. (The angles shown in these plots are the physical angles.) Indeed

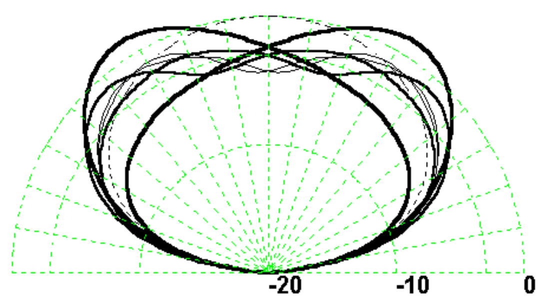

Fig. 2. Beampatterns for six element array with spacing λ/2 and an element coupling factor of $0.4\exp(j2\pi/3)$. The thick lines are the patterns for the two outside elements; the next thickest lines, the patterns for the next to outside elements; the thinnest lines, the patterns for the two inside elements. The dashed line is the expected pattern for no crosstalk.

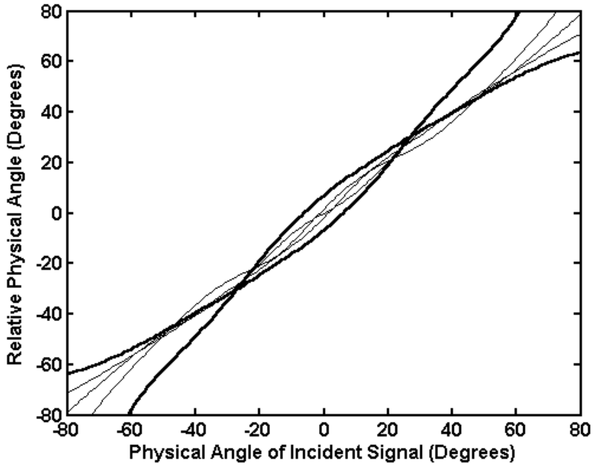

Fig. 3. Estimated relative physical angle between elements versus the relative angle of the incident signal for model array with crosstalk. The thick lines are the relative angles between the outside elements and the next inner elements. The thinner lines are the relative angles between the other inner elements.

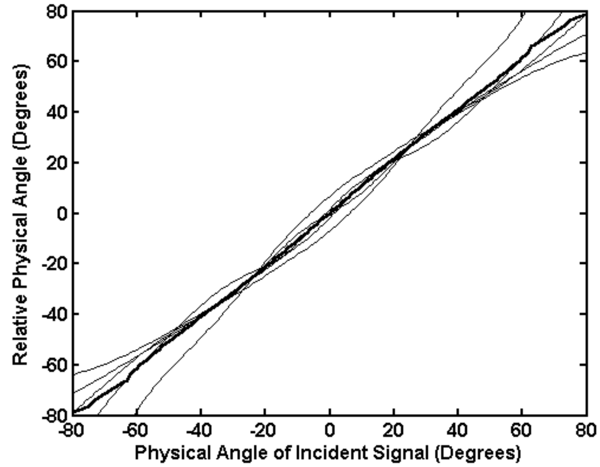

Fig. 4. Estimated relative physical angle between elements versus incident angle for model array with crosstalk. The thick line is the average of the five angle estimates.

for this situation the error in physical angle as measured from the relative physical angles in the region between –40 and 40^o is as large as ±8.6^o or as small as 0^o. The resulting error in spatial position about an arc at a given range can be expressed as a percentage of range by expressing the angle error in radians and multiplying by 100. For this example, the largest error is 8.6^o resulting in an error ratio of 15% which translates into a spatial error of 1.5 and 15m at ranges of 10 and 100 m respectively.

Another way of expressing the relative angle error and the method to be used later in the context of experimental arrays is by the standard deviation of the relative angles at each angle of incidence. For the six-element array characterized by the relative angles in Fig. 3 the average standard deviation between the incident angles of ±40^o is 3.18^o which results in an error ratio of 5.55%.

Since the array consists of six elements the angle estimation error can be reduced because there are five estimates of relative angle that can be averaged. Figure 4 shows the relative angles for all five two-element (adjacent) combinations and their average. A rough estimate of the variation of the mean can be obtained by dividing the average standard deviation by $\sqrt{5}$ because there are 5 combinations of two elements. (This procedure assumes the estimates are independent and identically distributed which they are not, but the procedure does provide a rough idea of the variation of the mean.) Hence we expect the mean to have an approximate standard deviation of $5.55\%/\sqrt{5} = 2.48\%$. This reduction in angle estimation error in the presence of crosstalk highlights the value of spatial smoothing in multi-angle swath bathymetry. In the case of only one signal arrival we can use five subarrays to form our estimate and, therefore, mitigate the effect of crosstalk.

If it were required to estimate the direction to two targets, say a primary target and a multipath, then each subarray must contain three elements. And from a six-element array there are four such subarrays and therefore there is also potential for crosstalk mitigation. Similarly, when solving for three targets, there are three four element subarrays, etc.

While the preceding discussion provides useful insight into the practical benefits of multi-angle swath bathymetry, the focus of this paper is on eliminating crosstalk rather than mitigating it, so attention is now turned to three experimental arrays.

III. PHYSICAL DESCRIPTION OF THREE EXPERIMENTAL ARRAYS

In this section we describe the structure for three arrays constructed to help understand and eliminate (as far as is practical) crosstalk. The three arrays, all resonant near 300 kHz, are shown in Fig. 5 and are denoted as array A, array B, and array C, from left to right. Illustrative crossections of each array are shown in Fig. 6. These crossections are drawn so as to emphasize certain features and therefore are not drawn to scale. The first array, array A, consists of twelve elements mounted in syntactic foam. The array housing is wide compared to the array. Only the centre six elements of the array are used for MASB with the three outside elements on each side used to make the crosstalk uniform over the centre six. It was hypothesised that if the array was identical from element to element, then the centre elements should, in theory, have very similar beampatterns and also relative angles. In other words, it is not necessarily a moderate level of crosstalk that is the problem but that the crosstalk causes non-uniform beampatterns and relative angles.

The second array, array B, was built with a smaller housing and constructed as a sandwich of elements and electrical insulation paper to provide isolation. The sandwich is mounted on similar paper and then to the housing. The space between the housing and the sandwich is filled with polyurethane. This array has one dummy element on either side of the six active elements. The dummy element on the right as pictured in Fig. 5 is made of aluminium rather than

Fig. 5. The three arrays used to explore the effects of crosstalk. Array A is on the left, array B is in the middle, and array C is on the right.

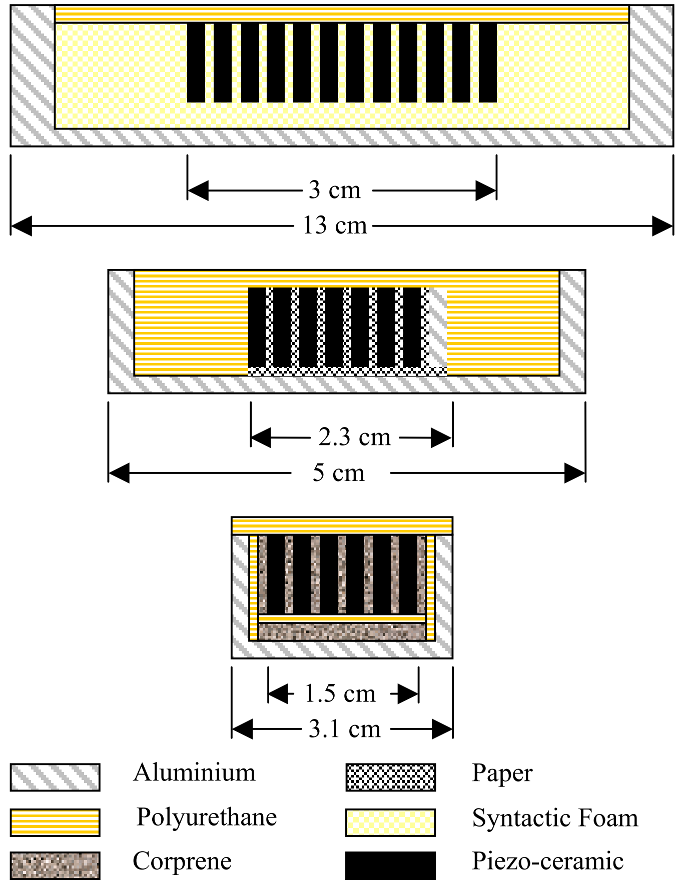

Fig. 6. Illustrative crossections (not to scale) of the three arrays, array A (top), array B (middle), and array C (bottom).

piezo-ceramic. This change in material was implemented to investigate the edge effect differences.

Both arrays A and B where not constructed in the Underwater Research Lab (URL) so the details of their structure and how they were built are not known except to the extent that such details can be determined after the fact.

Array C was built in the URL with the specific aim to minimize crosstalk. There are no dummy elements and the housing is relatively narrow. In addition, the housing edge and the elements are in the same plane (i.e. the elements are not recessed into the housing). The material between the elements is corprene [3].

IV. COHERENT BEAMPATTERNS

A. General Description

In the last section the physical structure of the three arrays was described. In this section the beampatterns and relative angle responses of these arrays are presented. The beampatterns and relative angle responses were measured using an eight channel coherent sonar controlling a stepper motor to rotate the arrays. The measurements were made in the URL's test tank at a separation of 3.8 m. The sonar pulse was transmitted from a separate stationary transducer mounted at the far side of the tank. The eight channel coherent sonar consists of eight custom-built variable-gain amplifiers, an eight channel A/D board (Interactive Circuits and Systems Ltd. (ICS), ICS-645 board), a four channel D/A board (ICS-660 board) and a high voltage transmitter. The D/A board produces the transmit waveform for the transmitter and the A/D board converts the array's received signals to digital form after they are conditioned by the amplifiers. The A/D and D/A boards run from the same clock and the trigger for the D/A board is derived from a sample frame synchronized trigger out of the A/D board. Therefore, the transmit waveform is always synchronized in phase with the sample times of the A/D board.

The frequency range of the amplifiers is from 30 kHz to about 700 kHz. Therefore, there is essentially no filtering on the front end except for the 700 kHz lowpass of the amplifiers. The sample rate for the 300 kHz carrier frequency was 1.2 MHz per channel implying four samples per carrier cycle. The digital signals were bandpass filtered with a filter width of 30 kHz and the pulse length was 100 carrier cycles. Since the samples are ¼ of a cycle apart, the inphase and quadrature components were obtained by retaining the sample pairs (1,2), (5,6), (9,10), etc.

The samples used to obtain the beampatterns and angle responses were those located in the steady state part of the pulse received. The decibel amplitude (beampattern) response was obtained by taking 10log the sum of the squared inphase and quadrature components. And the electrical phase angle was obtained by using the four-quadrant arctan of the quadrature component over the inphase component. The physical angle was determined from

$$\phi = \arcsin\left(\frac{\theta\lambda}{2\pi d}\right) \quad (6)$$

where ϕ is the physical angle, θ is the electrical phase angle, λ is the wavelength, and d is the spacing between elements.

Figure 7 shows the beampatterns and relative angle responses for array A, Fig. 8 for array B, and Fig. 9 for array C. The responses for all six elements are plotted in these figures to illustrate the variability.

For array A the beampattern and phase response vary rapidly with angle indicating that there is a degree of crosstalk from elements and/or structures far from the primary element (element being measured). More will be said later about the spatial extent of the interaction.

The variations in beampattern and phase response for array A are also large indicating that the crosstalk is large. In other words, there is little isolation between the elements and/or structures comprising the array.

It is evident that although the array was designed to be uniform and there were twelve elements and only the centre six were used, the resulting patterns were not uniform. The lack of uniformity indicates that in spite of the careful design

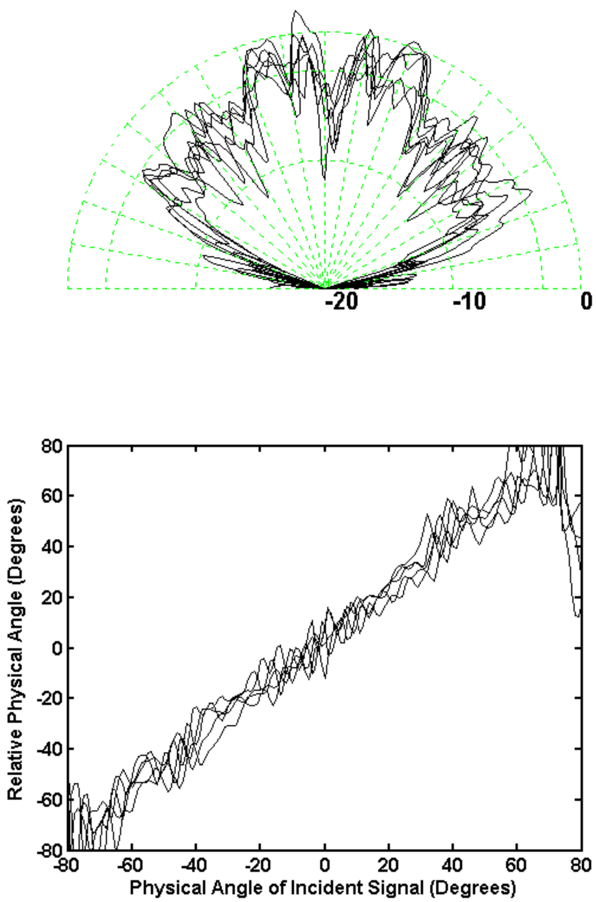

Fig. 7. Beampatterns (top) and relative physical angle response (bottom) for array A.

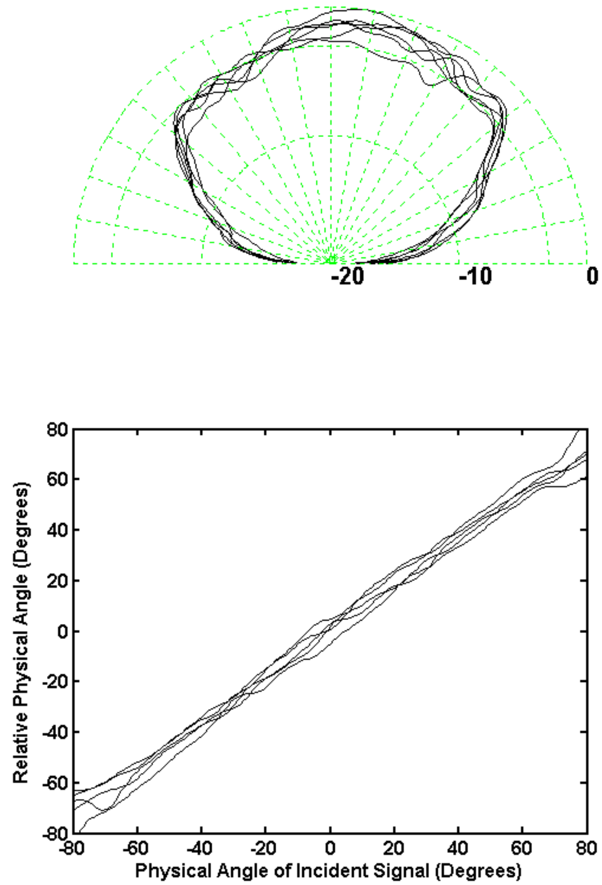

Fig. 8. Beampatterns (top) and relative physical angle response (bottom) for array B.

and construction acoustically speaking the array is not uniform.

Similar results are evident in the patterns for array B. The major difference between the patterns for array B and array A is that the rapid variations with angle are replaced by slower variations. The fact that the variations are less rapid indicates that the contributing crosstalk structures are not spread spatially to the extent that they are in array A. The magnitudes of the variations are again fairly large indicating that the primary element is not effectively isolated from the crosstalk inducing structures.

Although the beampatterns for array B appear to lean to the right it is hard to tell whether this response is partly due to the aluminium dummy element or to a twisting of the array sandwich as it was constructed. The variation in response with angle is quite large and hence probably masks the effect of the inconsistent dummy element.

The beampatterns and phase responses for array C are quite smooth and the amplitude of the variations is quite small. Two of the responses have maximums, one to the right of centre and one to the left of centre and these responses also budge to the opposite sides at low and high angles. These are the responses for the end elements and it is

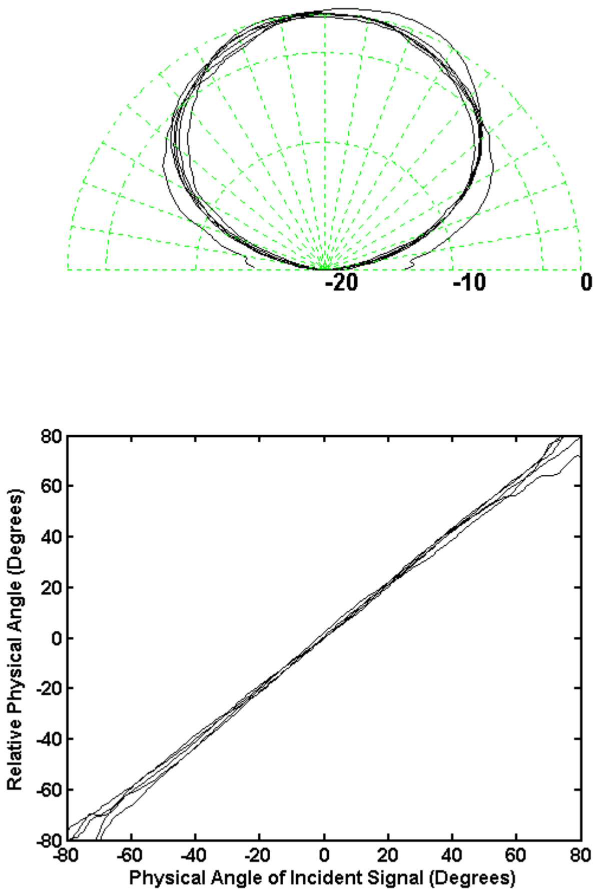

Fig. 9. Beampatterns (top) and relative physical angle response (bottom) for array C.

assumed the offset maximums are due to the fact that there are no neighbouring elements on one side of these primary elements. The lack of symmetry in the response of the end elements indicates there is crosstalk between elements. But because the lack of symmetry is not evident for the inside elements the crosstalk appears to be confined chiefly to neighbouring elements and there is little or no contribution from distant elements or structures in the array.

B. Spatial Extent of Crosstalk

From the rapid variation in the beampatterns for arrays A and B and particularly A, it is evident that the source of crosstalk is spatially spread. In other words, as the array is rotated sources of crosstalk that are farther away from the primary element should give rise to higher frequency components in the pattern's ripple. Taking the inverse Fourier transform of the far field pattern gives the distribution of crosstalk sources across the array. This distribution or aperture function is masked somewhat by the fact that the inverse Fourier transform can be taken only of the visible region of the array response and is also subject to the shaping factor $\cos\phi$. Therefore, the resolution of the aperture function is limited by the shape of the inverse Fourier transform of the equivalent pattern in wavenumber space of $\cos\phi$. This limiting aperture function is convolved with the actual aperture function to yield a filtered or smoothed result.

Figure 10 shows the expected result for six elements of an array with spacing 0.25 cm ($\lambda/2$ at 300 kHz) assuming each element has a perfect $\cos\phi$ beam shape. As a reference, the insert in the figure shows the aperture function for one element. In establishing the approximate spatial spread of crosstalk sources we note differences from the group of six ideal aperture functions shown in Fig. 10.

Figure 11 shows the aperture function for arrays A, B, and C. The aperture functions for all six elements of each are plotted together to show the displacement of the element centres and the total extent of the significant part of the total distribution. The aperture functions for all three arrays show concentrations around the element positions that drop off rapidly to a level of –16 dB which is consistent with the level of the first sidelobe (–18 dB) of the ideal aperture function. From this level the aperture functions of arrays B and C, which are the narrower arrays (5 cm and 3.1 cm repectively), fall off in a similar manner as do the ideal, but the aperture function of array B reaches a floor of about –42 dB whereas the floor for array C is –50 dB. This difference in the floor level and the fact that the functions for array B tend to be more random than those for array C probably indicates that array B has a higher degree of unsystematic acoustic properties.

The aperture functions for array A have a higher floor level (–38 to –40 dB) than those for either arrays B or C and the functions are also less regular indicating again that this array probably has a high degree of unsystematic acoustic properties despite its apparent uniform construction. The aperture functions for array A are also much broader than those for arrays B and C. In fact, the functions for array A are about 12.5 cm wide at the –30 dB level as compared to 4.5 cm for arrays B and C. This apparent width of the aperture function for array A of 12.5 cm is very close to the actual width of the transducer face of 12.7 cm. Therefore, it

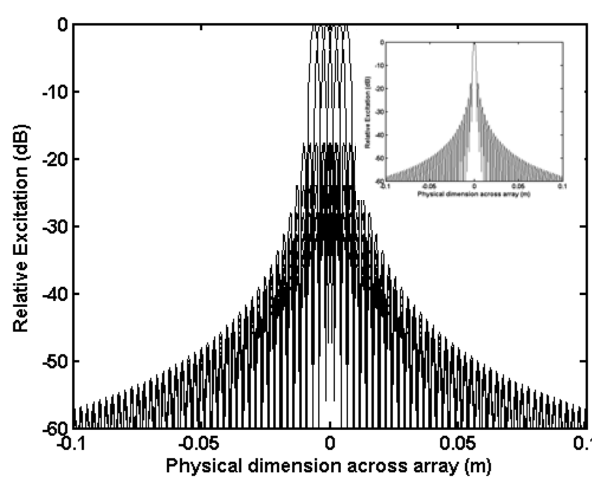

Fig. 10. Expected spatial aperture functions for six elements of an array with spacing 0.25 cm assuming each element has a perfect $\cos\phi$ beam shape. Insert is the spatial aperture function for a single element.

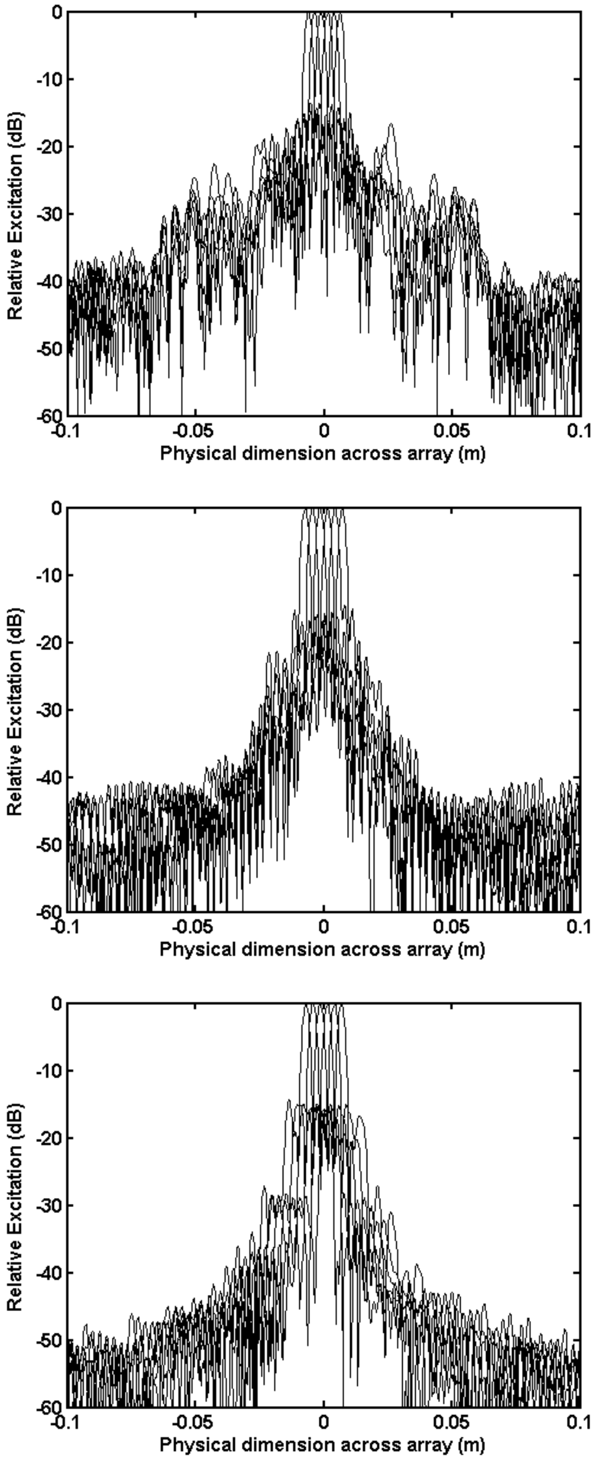

Fig. 11. Spatial aperture functions for array A (top), array B (middle), and array C (bottom).

is concluded that a good deal of the broad face of array A is acoustically active and contributes to the less than ideal beampatterns measured for this array.

C. Phase Response and Angle Accuracy

Angle estimates are made from the phase differences across the array. For multiple angles the angle estimates must obtained by least squares techniques resulting in complex solutions that do not provide much light on the effects of crosstalk. But for a single angle the accuracy is readily predicted from the relative angle responses shown in Figs. 7, 8, and 9 for arrays A, B, and C respectively. Table 1 shows the average (averaged from –40 to +40^o) relative angle error expressed as a percentage of range for the three arrays. Also shown is the expected standard deviation of the average of all five angle errors assuming that the variations at a particular angle are uncorrelated. This assumption is obviously not true but the result does give an indication of the magnitude of the improvement that might be expected using multiple subarrays. These angle errors are equivalent to the angular spread expressed in radians multiplied by 100. Multiplying this ratio by the range gives the arc length of the spatial spread at that range.

This table indicates the kind of angle estimation performance expected for a two and then six element array with the associated levels of crosstalk. In other words, if the array were used to estimate the angle to a single target (i.e. no multiple arrivals), these are the errors expected. Since the array has six elements it is possible to combine five two-element subarrays to reduce the effect of the crosstalk. For example, array A has severe crosstalk and housing interactions and the resulting standard deviation in the physical angle for two elements is 4.87^o. Therefore, the spatial (length along and arc) standard deviation-to-range ratio is 8.5% (i.e. the standard deviation of the angle expressed in radians and then as a percent of the radius). This translates into a physical distance spread about an arc of 0.85 m at a range of 10 m and 8.5 m at a range of 100 m. But if all six elements are used to estimate angle and if our assumption that the standard deviation in the error can at least be approximated by a reduction of about square root of 5 (square root of the number of two element subarrays), then the error standard deviation to range ratio drops to 3.8%.

TABLE 1
STANDARD DEVIATION OF EXPECTED SPATIAL SPREAD AS A PERCENT OF RANGE

Array	d/λ	Standard Deviation, % of Range	
		Single pair	Average of pairs
A	0.5	8.5	3.8
B	0.607	4.9	2.2
C	0.543	1.9	0.9

For array B with the smaller housing and smoother relative angle response the ratio of error standard deviation to range for two elements is 4.9% and reduces to 2.2% if all six elements are used to estimate angle. Array C having the least crosstalk and housing interaction, and therefore the smoothest relative angle response also has the least two-element error to range ratio, 1.9%. And if all six elements are used to estimate angle, the ratio drops to 0.9%. This ratio translates into a crosstalk-induced standard deviation in the arc length at a range of 100 m of only 0.9 m.

V. CONCLUSIONS

In this paper we presented the beampatterns and relative physical angle responses of three six element arrays designed for MASB applications. Variations across the beampatterns indicated that the arrays all suffered from varying degrees of crosstalk. Array A, constructed with a relatively large face, syntactic foam between elements, and three dummy elements on either side of the active six, had the largest degree of crosstalk. Array B, constructed with a smaller face, insulation paper between elements, and one dummy element on either side of the six active elements, had similar levels of crosstalk, but the crosstalk sources were not so widely distributed. Array C, constructed with a small face, corprene between elements, and only six elements, had the lowest level of crosstalk and this crosstalk also did not appear to be coming from widely separated sources.

In practical applications the materials used in constructing an array must also be suitable for the environment the array will be used in. The corprene in array C proved effective at reducing crosstalk but its compressablity limits the depth. The syntactic foam used to construct array A, on the other hand, has low compressibilty and therefore the array can be used at greater depth.

Future research will aim at developing tools to measure the suitability of arrays for MASB applications and designing practical arrays that reduce the effect of crosstalk on angle estimation. The research will focus on developing the coherent beampattern approach to array performance evaluation for MASB applications. Variation of operating frequency with respect to the series and parallel resonance of transducer elements will be explored along with the influence of housing structures. The potential for the aperture function to yield information about acoustic performance will also be further investigated.

Acknowledgments

The authors acknowledge with thanks the support of the Natural Science and Engineering Research Council (NSERC) in Canada, the Advanced Systems Institute of B.C., and International Submarine Engineering Ltd.

References

[1] P. Kraeutner, J.S. Bird, (SFU), D. Bishop, B. Charbonneau, F. Hegg, (Benthos Inc.), "Multi-Angle swath bathymetry sidescan qualitative performance Analysis," *Oceans'2002*, Bilox, Mississippi, October 29-31, 2002, pp. 1234-1244.

[2] B. Delannoy, H. Lasota, C. Bruneel, R. Torguet, and E. Bridoux, "The infinite baffles problem in acoustic radiation and its experimental verification," *J. Appl. Phys.* 50(8), August 1979, pp 5189-5195.

[3] R.W. Higgs, and L.J. Eriksson, "Acoustic Decoupling Properties of Corprene DC-100," *Journal of the Acoustical Society of America*, 46(5, part 2), 1969, pp. 1254-1258.